

State-insensitive trapping of Rb atoms: Linearly versus circularly polarized light

Bindiya Arora

Department of Physics, Guru Nanak Dev University, Amritsar, Punjab-143005, India

B. K. Sahoo*

Theoretical Physics Division, Physical Research Laboratory, Ahmedabad-380009, India

(Received 18 July 2012; published 17 September 2012)

We study the cancellation of differential ac Stark shifts in the $5s$ and $5p$ states of the rubidium atom using the linearly and circularly polarized lights by calculating their dynamic polarizabilities. Matrix elements were calculated using a relativistic coupled-cluster method at the single and double excitations and at the important valence triple excitation approximation including all possible nonlinear correlation terms. Some of the important matrix elements were further optimized using the experimental results available for the lifetimes and static polarizabilities of atomic states. “Magic wavelengths” are determined from the differential Stark shifts and results for the linearly polarized light are compared with the previously available results. The possible scope of facilitating state-insensitive optical trapping schemes using the magic wavelengths for circularly polarized light is discussed. Using the optimized matrix elements, the lifetimes of the $4d$ and $6s$ states of this atom are ameliorated.

DOI: [10.1103/PhysRevA.86.033416](https://doi.org/10.1103/PhysRevA.86.033416)

PACS number(s): 32.60.+i, 37.10.Jk, 32.10.Dk, 32.70.Cs

I. INTRODUCTION

The investigation of the properties of the rubidium (Rb) atom is of immense interest for a number of applications [1–11]. It is one of the most widely used atoms in quantum computational schemes using Rydberg atoms, where the hyperfine states of the ground state of the Rb atom are defined as the qubits [4]. It is also used to study quantum phase transitions of mixed species with degenerate quantum gases [6]. There are several proposals to carry out precision studies in this atom, such as constructing ultraprecise atomic clocks [7–9], probing parity nonconservation effects [10], finding its permanent electric dipole moment [11], etc. Also, a number of measurements and calculations of lifetimes for many low-lying states in Rb have been performed over the past few decades [12–18]. It is found that there are inconsistencies between the calculated and measured values of the lifetimes of atomic states in this atom [18]. In this context, it is necessary to carry out further theoretical studies of this atom.

Due to the simple single-core electron structure of this atom, it is adequate to employ advanced many-body methods for the precise calculation of its properties, which ultimately act as benchmark tests for the experimental measurements [19–21]. In this paper, we determine the polarizabilities of the ground $5s$ and excited $5p$ states and study the differential ac Stark shifts between these two states. In this process, we also analyze the reduced matrix elements and their accuracies, which are further used to estimate precisely the lifetimes of few excited states in this atom. The aim of our present study is to analyze results of differential ac Stark shifts from which we can deduce the magic wavelengths (see below for definition) that are of great use in the state-insensitive trapping of Rb atoms.

The manipulation of cold and ultracold Rb atoms has been widely done by using optical traps [22,23]. For a number of applications (such as atomic clocks and quantum computing

[24,25]), it is often desirable to optically trap the neutral atoms without affecting the internal energy-level spacing for the atoms. However, in an experimental setup, the interaction of an atom with the externally applied oscillating electric field of the trapping beam inevitably causes ac Stark shifts of the atomic levels. For any two internal states of an atom, the Stark shifts caused by the trap light are, in general, different, which affects the fidelity of the experiments [26,27]. Katori *et al.* [28] proposed the idea of tuning the trapping laser to a magic wavelength, “ λ_{magic} ,” at which the differential ac Stark shifts of the transition are terminated. Using this approach, the magic wavelength for the $5s^2\ ^1S_0^0-5s5p\ ^3P_0^0$ transition in ^{87}Sr was determined with a high precision to be 813.42735(40) nm [29]. McKeever *et al.* demonstrated the state-insensitive trapping of Cs at $\lambda_{\text{magic}} \approx 935$ nm, while still maintaining a strong coupling with the $6s_{1/2}-6p_{3/2}$ transition [30]. Arora *et al.* [31] calculated the magic wavelengths for the $np-ns$ transitions for other alkali-metal atoms (from Na to Cs) by calculating dynamic polarizabilities using a relativistic coupled-cluster (RCC) method. Theoretical values for these quantities were calculated at wavelengths where the ac polarizabilities for two states involved in the transition cancel. The data in Ref. [31] provide a wide range of magic wavelengths for the alkali-metal atoms trapped in linearly polarized light by evaluating electric dipole (E1) matrix elements obtained by the linearized RCC method. In this paper, we try to evaluate these matrix elements considering all possible nonlinear terms in the RCC method. In addition, we would like to optimize the matrix elements using the precisely known experimental results of lifetimes and static polarizabilities for different atomic states and reinvestigate the above-reported magic wavelengths in the considered atom. It is also reported in Ref. [31] that trapping Rb atoms in the linearly polarized light offers only a few suitable magic wavelengths for the state-insensitive scheme. This persuades us to look for more plausible cases for constructing state-insensitive traps of Rb atoms using the circularly polarized light. Using the circularly polarized light may be advantageous owing to the dominant role played by vector polarizabilities (which are

*bijaya@prl.res.in

absent in the linearly polarized light) in estimating the ac Stark shifts. Moreover, these vector polarizabilities act as “fictitious magnetic fields,” turning the ac Stark shifts to the case analogous to the Zeeman shifts [32,33].

This paper is organized as follows. In Secs. II and III, we briefly discuss the theory of dipole polarizability and the method used for calculating them precisely. In Sec. IV, we first discuss in detail the evaluation of the matrix elements used for the precise estimation of polarizability and then present our magic wavelengths first for the linearly polarized light and then for the circularly polarized light. Unless stated otherwise, we use the conventional system of atomic units (a.u.), in which e , m_e , $4\pi\epsilon_0$, and the reduced Planck constant \hbar have the numerical value 1 throughout this paper.

II. THEORY OF DIPOLE POLARIZABILITY

The v th energy level of an atom placed in a static electric field \mathcal{E} can be expressed using a time-independent perturbation theory as [34]

$$E_v = E_v^0 + \sum_{k \neq v} \frac{|\langle \psi_v | V | \psi_k \rangle|^2}{E_v^0 - E_k^0} + \dots, \quad (1)$$

where E_i^0 s are the unperturbed energy levels in the absence of electric field, k represent the intermediate states allowed by the dipole selection rules, and $V = -D \cdot \mathcal{E}$ is the interaction Hamiltonian with D as the electric dipole operator. Since the first-order correction to the energy levels is zero in the present case, we can approximate the energy shift at the second-order level for a weak field \mathcal{E} and write it in terms of dipole moments p as

$$\Delta E_v = E_v - E_v^0 \simeq \sum_{k \neq v} \frac{(p^*)_{vk}(p)_{kv}}{\delta E_{vk}} \mathcal{E}^2, \quad (2)$$

where $\delta E_{vk} = (E_v^0 - E_k^0)$, and $(p)_{vk} = \langle \psi_v | D | \psi_k \rangle$ is the E1 amplitude between the $|\psi_v\rangle$ and $|\psi_k\rangle$ states. A more traditional notation of the above equation is given by

$$\Delta E_v = -\frac{1}{2} \alpha_v \mathcal{E}^2, \quad (3)$$

where α_v is known as the static polarizability of the v th state, which is written as

$$\alpha_v = -2 \sum_{k \neq v} \frac{(p^*)_{vk}(p)_{kv}}{\delta E_{vk}}. \quad (4)$$

If the applied field is frequency dependent (ac field), then we can still express the change in energy as $\Delta E_v = -\frac{1}{2} \alpha_v \mathcal{E}^2$, with α_v as a function of frequency given by

$$\alpha_v(\omega) = - \sum_{k \neq v} (p^*)_{vk}(p)_{kv} \left[\frac{1}{\delta E_{vk} + \omega} + \frac{1}{\delta E_{vk} - \omega} \right]. \quad (5)$$

Since $\alpha_v(\omega)$ also depends on angular momentum j and m_j values of the given atomic state, it is customary to express them in a different form with m_j dependent factors and m_j independent factors. Therefore, $\alpha_v(\omega)$ is further rewritten

as [35]

$$\alpha_v(\omega) = \alpha_v^0(\omega) + \mathcal{A} \cos \theta_k \frac{m_j}{j} \alpha_v^1(\omega) + \left\{ \frac{3 \cos^2 \theta_p - 1}{2} \right\} \frac{3m_j^2 - j(j+1)}{j(2j-1)} \alpha_v^2(\omega), \quad (6)$$

where \mathcal{A} , θ_k , and θ_p define the degree of circular polarization, the angle between the wave vector of the electric field and the z axis, and the angle between the direction of polarization and the z axis, respectively. Here, $\mathcal{A} = 0$ for the linearly polarized light, which implies that there is no vector component present in this case; otherwise, $\mathcal{A} = 1$ for the right-handed and $\mathcal{A} = -1$ for the left-handed circularly polarized light. In the absence of magnetic field (or in weak magnetic field), we can choose $\cos(\theta_k) = \cos(\theta_p) = 1$. Here, m_j independent factors α_v^0 , α_v^1 , and α_v^2 are known as scalar, vector, and tensor polarizabilities, respectively. In terms of the reduced matrix elements of the dipole operator, they are given by Ref. [35]

$$\alpha_v^0(\omega) = \frac{1}{3(2j_v + 1)} \sum_{j_k} |\langle \psi_v || D || \psi_k \rangle|^2 \times \left[\frac{1}{\delta E_{kv} + \omega} + \frac{1}{\delta E_{kv} - \omega} \right], \quad (7)$$

$$\alpha_v^1(\omega) = -\sqrt{\frac{6j_v}{(j_v + 1)(2j_v + 1)}} \sum_{j_k} \begin{Bmatrix} j_v & 1 & j_v \\ 1 & j_k & 1 \end{Bmatrix} \times (-1)^{j_v + j_k + 1} |\langle \psi_v || D || \psi_k \rangle|^2 \times \left[\frac{1}{\delta E_{kv} + \omega} - \frac{1}{\delta E_{kv} - \omega} \right], \quad (8)$$

$$\alpha_v^2(\omega) = -2\sqrt{\frac{5j_v(2j_v - 1)}{6(j_v + 1)(2j_v + 1)(2j_v + 3)}} \times \sum_{j_k} \begin{Bmatrix} j_v & 2 & j_v \\ 1 & j_k & 1 \end{Bmatrix} (-1)^{j_v + j_k + 1} |\langle \psi_v || D || \psi_k \rangle|^2 \times \left[\frac{1}{\delta E_{kv} + \omega} + \frac{1}{\delta E_{kv} - \omega} \right]. \quad (9)$$

For $\omega = 0$, the results will correspond to the static polarizabilities, which clearly suggests that α_v^1 is zero for the static case.

III. METHOD OF CALCULATIONS

To calculate wave functions in an Rb atom, we first obtain the Dirac-Fock (DF) wave function for the closed-shell configuration $[4p^6]$, which is given by $|\Phi_0\rangle$. Then the DF wave function for atomic states with one valence configuration is defined as

$$|\Phi_v\rangle = a_v^\dagger |\Phi_0\rangle, \quad (10)$$

where a_v^\dagger represents the addition of the valence orbital, denoted by v , with $|\Phi_0\rangle$. The exact atomic wave function ($|\Psi_v\rangle$) for such a configuration is determined, accounting for correlation effects in the RCC framework, by the expression [36]

$$|\Psi_v\rangle = e^T \{1 + S_v\} |\Phi_v\rangle, \quad (11)$$

which in linear form is given by

$$|\Psi_v\rangle \approx \{1 + T + S_v\}|\Phi_v\rangle. \quad (12)$$

Here, T and S_v operators account for the excitations of the electrons from the core orbitals alone and from the valence orbital together with core orbitals, respectively. In the present paper, we consider Eq. (11) instead of Eq. (12) as was taken before in our previous calculations [31]. We consider here only coupled-cluster single and double excitations (the CCSD method) and important triple excitations [known as the CCSD(T) method from $|\Phi_v\rangle$].

The excitation amplitudes for the T operators are determined by solving

$$\langle\Phi_0^*|\{\widehat{H}e^T\}|\Phi_0\rangle = 0, \quad (13)$$

where $|\Phi_0^*\rangle$ represents singly and doubly excited configurations from $|\Phi_0\rangle$. Similarly, the excitation amplitudes for the S_v operators are determined by solving

$$\langle\Phi_v^*|\{\widehat{H}e^T\}\{1 + S_v\}|\Phi_v\rangle = \langle\Phi_v^*|S_v|\Phi_v\rangle\Delta E_v^{\text{att}}, \quad (14)$$

taking $|\Phi_v^*\rangle$ as the singly and doubly excited configurations from $|\Phi_v\rangle$. The above equation is solved simultaneously with the calculation of attachment energy ΔE_v^{att} for the valence electron v using the expression

$$\Delta E_v^{\text{att}} = \langle\Phi_v|\{\widehat{H}e^T\}\{1 + S_v\}|\Phi_v\rangle. \quad (15)$$

The triples effect is incorporated through the calculation of ΔE_v^{att} by including valence triple excitation amplitudes perturbatively (e.g., see [37] for a detailed discussion).

To determine polarizabilities, we divide various correlation contributions to it into three parts as

$$\alpha_v^\lambda = \alpha_v^\lambda(c) + \alpha_v^\lambda(vc) + \alpha_v^\lambda(v), \quad (16)$$

where $\lambda = 0, 1, \text{ and } 2$ represent scalar, vector, and tensor polarizabilities, respectively, and the notations c , vc , and v in the parentheses correspond to core, core-valence, and valence correlations, respectively. The core contributions to the vector and tensor polarizabilities are zero.

We determine the valence correlation contributions to the polarizability in the sum-over-states approach [38] by evaluating their matrix elements by our CCSD(T) method and using the experimental energies [39–41] for the important intermediate states. Contributions from the higher excited states and continuum are accounted for by the following expression:

$$\alpha_v^\lambda = C_\lambda \langle\Psi_v|D|\Psi_v^{(1)}\rangle, \quad (17)$$

where C_λ are the corresponding angular factors for different values of λ , and $|\Psi_v^{(1)}\rangle$ is treated as the first-order wave function to $|\Psi_v\rangle$ due to the dipole operator D [42] at the third-order many-body perturbation [the MBPT(3) method] level and given as $\alpha_v^\lambda(\text{tail})$. Also, contributions from the core and core-valence correlations are estimated using this procedure.

We calculate the reduced matrix elements of D between states $|\Psi_f\rangle$ and $|\Psi_i\rangle$, to be used in the sum-over-states approach, from the following RCC expression:

$$\langle\Psi_f||D||\Psi_i\rangle = \frac{\langle\Phi_f||\{1 + S_f^\dagger\}\overline{D}\{1 + S_i\}||\Phi_i\rangle}{\sqrt{\mathcal{N}_f\mathcal{N}_i}}, \quad (18)$$

where $\overline{D} = e^{T^\dagger}De^T$ and $\mathcal{N}_v = \langle\Phi_v|e^{T^\dagger}e^T + S_v^\dagger e^{T^\dagger}e^T S_v|\Phi_v\rangle$ involve two nontruncating series in the above expression. The calculation procedures of these expressions are discussed in detail elsewhere [43,44].

IV. RESULTS AND DISCUSSION

Our aim is to determine the magic wavelengths for the linearly and circularly polarized electric fields for the $5s$ – $5p_{1/2,3/2}$ transitions in the Rb atom. To determine these wavelengths precisely, we need accurate values of polarizabilities, which depend upon the excitation energies and the E1 matrix elements between the intermediate states of the corresponding states. In this respect, we first present below the E1 matrix elements between different transitions and discuss their accuracies. Then we present an overview of the current status of the polarizabilities reported in the literature and compare our results with them. These results are further used to determine the magic wavelengths for both the linearly and circularly polarized lights.

A. Matrix elements

The matrix elements of the Rb atom have been reported several times previously [11,18,26,31,45–48]. We present these results from our calculations in Table I using the DF and CCSD(T) methods; the differences in the results imply the amount of correlation effects involved to evaluate these matrix elements. We also give uncertainties in the CCSD(T) results mentioned in the parentheses in the same table. The contributions to these uncertainties come from the neglected triple excitations in the RCC method and from the incompleteness of the used basis functions. The uncertainty contribution from the former is estimated from the differences between the CCSD and CCSD(T) results. Some of the important matrix elements are determined more precisely below from the available experimental lifetime results of atomic states involving only one (strong) transition channel. However, in case there is more than one (strong) decay channel associated with an atomic state, it would be an intricate procedure to obtain the matrix elements precisely, but it has been done by optimizing these values to reproduce the experimental lifetimes in conjunction with the experimental static polarizabilities of different atomic states, as discussed below.

In order to evaluate the magnitude of the $5s \rightarrow 5p_{1/2}$ E1 transition matrix element, we use the measured lifetime of the $5p_{1/2}$ state, which was reported as 27.75(8) ns in Ref. [50]. Using the fact that the $5p_{1/2}$ state decays only to the $5s$ state, the line strength of the $5s \rightarrow 5p_{1/2}$ transition can be obtained by combining this measured lifetime with the experimental wavelength ($\lambda = 7949.8 \text{ \AA}$) of the corresponding transition. The value of the E1 matrix element of the $5s \rightarrow 5p_{1/2}$ transition is obtained from this result as 4.227(6) a.u. Similarly, it is possible to deduce the magnitude of the E1 matrix element of the $5s \rightarrow 5p_{3/2}$ transition by combining the measured lifetime of the $5p_{3/2}$ state, reported as 26.25(8) ns [50], with its experimental wavelength (7802.4 \AA). However, the $5p_{3/2}$ state has nonzero transition probabilities to the $5s$ and $5p_{1/2}$ states via the allowed E1 and the forbidden M1 and E2 channels. We found from our calculations that the transition

TABLE I. Absolute values of E1 matrix elements in the Rb atom in ea_0 using the Dirac-Fock (DF) and CCSD(T) methods. Uncertainties in the CCSD(T) results are given in parentheses.

Transition	DF	CCSD(T)
$5s_{1/2} \rightarrow 5p_{1/2}$	4.819	4.26(3)
$5s_{1/2} \rightarrow 6p_{1/2}$	0.382	0.342(2)
$5s_{1/2} \rightarrow 7p_{1/2}$	0.142	0.118(1)
$5s_{1/2} \rightarrow 8p_{1/2}$	0.078	0.061(5)
$5s_{1/2} \rightarrow 9p_{1/2}$	0.052	0.046(3)
$5s_{1/2} \rightarrow 5p_{3/2}$	6.802	6.02(5)
$5s_{1/2} \rightarrow 6p_{3/2}$	0.605	0.553(3)
$5s_{1/2} \rightarrow 7p_{3/2}$	0.237	0.207(2)
$5s_{1/2} \rightarrow 8p_{3/2}$	0.135	0.114(2)
$5s_{1/2} \rightarrow 9p_{3/2}$	0.091	0.074(2)
$5p_{1/2} \rightarrow 6s_{1/2}$	4.256	4.144(3)
$5p_{1/2} \rightarrow 7s_{1/2}$	0.981	0.962(4)
$5p_{1/2} \rightarrow 8s_{1/2}$	0.514	0.507(3)
$5p_{1/2} \rightarrow 9s_{1/2}$	0.337	0.333(1)
$5p_{1/2} \rightarrow 10s_{1/2}$	0.239	0.235(1)
$5p_{1/2} \rightarrow 4d_{3/2}$	9.046	8.07(2)
$5p_{1/2} \rightarrow 5d_{3/2}$	0.244	1.184(3)
$5p_{1/2} \rightarrow 6d_{3/2}$	0.512	1.002(3)
$5p_{1/2} \rightarrow 7d_{3/2}$	0.447	0.75(2)
$5p_{1/2} \rightarrow 8d_{3/2}$	0.366	0.58(2)
$5p_{1/2} \rightarrow 9d_{3/2}$	0.304	0.45(1)
$5p_{3/2} \rightarrow 6s_{1/2}$	6.186	6.048(5)
$5p_{3/2} \rightarrow 7s_{1/2}$	1.392	1.363(4)
$5p_{3/2} \rightarrow 8s_{1/2}$	0.726	0.714(3)
$5p_{3/2} \rightarrow 9s_{1/2}$	0.476	0.468(2)
$5p_{3/2} \rightarrow 10s_{1/2}$	0.338	0.330(2)
$5p_{3/2} \rightarrow 4d_{3/2}$	4.082	3.65(2)
$5p_{3/2} \rightarrow 5d_{3/2}$	0.157	0.59(2)
$5p_{3/2} \rightarrow 6d_{3/2}$	0.255	0.48(2)
$5p_{3/2} \rightarrow 7d_{3/2}$	0.217	0.355(4)
$5p_{3/2} \rightarrow 8d_{3/2}$	0.176	0.272(3)
$5p_{3/2} \rightarrow 9d_{3/2}$	0.145	0.212(2)
$5p_{3/2} \rightarrow 4d_{5/2}$	12.24	10.96(4)
$5p_{3/2} \rightarrow 5d_{5/2}$	0.493	1.76(3)
$5p_{3/2} \rightarrow 6d_{5/2}$	0.778	1.42(3)
$5p_{3/2} \rightarrow 7d_{5/2}$	0.658	1.06(2)
$5p_{3/2} \rightarrow 8d_{5/2}$	0.530	0.81(1)
$5p_{3/2} \rightarrow 9d_{5/2}$	0.417	0.593(5)

probabilities through the forbidden channels are very small and negligibly influence the lifetime of the $5p_{3/2}$ state; in fact, it lies within the reported experimental error bar. Neglecting these contributions, we extract the E1 matrix element of the $5s \rightarrow 5p_{3/2}$ transition to be 5.977(9) a.u.

The estimated E1 matrix elements for the $5s-5p$ transitions from the experimental data are in close agreement with our calculated results within the predicted uncertainties. These results are further used, along with other matrix elements obtained from the CCSD(T) method, to calculate the polarizabilities of the $5s$ and $5p$ states. In Table II, we list the polarizability of the $5s$ state as 318.3(6) a.u., along with the detailed breakdown of the various contributions. The most precise experimental result reported for this quantity as 318.79(1.42) a.u. [51] is in excellent agreement with our result. As shown in Table II, the dominant contributions to

TABLE II. Scalar polarizability of the $5s$ state in Rb (in a.u.). Uncertainties in the results are given in parentheses.

Contribution	E1 amplitude	Contribution to α_v^0
$\alpha_{5s_{1/2}}(v)$		
$5s_{1/2} \rightarrow 5p_{1/2}$	4.227(6)	103.92(1)
$5s_{1/2} \rightarrow 6p_{1/2}$	0.342(2)	0.361
$5s_{1/2} \rightarrow 7p_{1/2}$	0.118(1)	0.037
$5s_{1/2} \rightarrow 8p_{1/2}$	0.061(5)	0.009
$5s_{1/2} \rightarrow 9p_{1/2}$	0.046(3)	0.005
$5s_{1/2} \rightarrow 5p_{3/2}$	5.977(9)	203.92(4)
$5s_{1/2} \rightarrow 6p_{3/2}$	0.553(3)	0.940
$5s_{1/2} \rightarrow 7p_{3/2}$	0.207(2)	0.112
$5s_{1/2} \rightarrow 8p_{3/2}$	0.114(2)	0.032
$5s_{1/2} \rightarrow 9p_{3/2}$	0.074(2)	0.013
$\alpha_{5s_{1/2}}(c)$		9.1(5)
$\alpha_{5s_{1/2}}(vc)$		-0.26(2)
$\alpha_{5s_{1/2}}(\text{tail})$		0.11(1)
Total		318.3(6)

the $5s$ state polarizability are from the $5s-5p$ transitions following a significant contribution from the core correlation. We have calculated the core-correlation contribution using the MBPT(3) method and the given uncertainty is estimated by scaling the wave functions. Our result for the core contribution is in very good agreement with the result obtained using the random-phase approximation (RPA) [52]. The consistency in the estimated $5s$ polarizability value obtained using the $5s \rightarrow 5p_{1/2}$ and $5s \rightarrow 5p_{3/2}$ matrix elements, which are obtained from the experimental lifetimes of the $5p$ states, and the experimental polarizability result suggests that both of these matrix elements are very accurate. In order to test the accuracy of our results further, we reproduce the dynamic polarizability of the $5s$ state at $\lambda = 1064$ nm, whose experimental value is reported as 769(61) a.u. [49]. As shown in Table III, our result shows a large discrepancy with the experimental measurement. Even after replacing the above E1 matrix elements with

TABLE III. Dynamic polarizability of the $5s$ state in Rb (in a.u.) at $\lambda = 1064$ nm. Uncertainties in the results are given in parentheses.

Contribution	E1 amplitude	Contribution to α_v^0
$\alpha_{5s_{1/2}}(v)$		
$5s_{1/2} \rightarrow 5p_{1/2}$	4.227(6)	235.24(3)
$5s_{1/2} \rightarrow 6p_{1/2}$	0.342(2)	0.428
$5s_{1/2} \rightarrow 7p_{1/2}$	0.118(1)	0.041
$5s_{1/2} \rightarrow 8p_{1/2}$	0.061(5)	0.010
$5s_{1/2} \rightarrow 9p_{1/2}$	0.046(3)	0.006
$5s_{1/2} \rightarrow 5p_{3/2}$	5.977(9)	441.14(8)
$5s_{1/2} \rightarrow 6p_{3/2}$	0.553(3)	1.114
$5s_{1/2} \rightarrow 7p_{3/2}$	0.207(2)	0.127
$5s_{1/2} \rightarrow 8p_{3/2}$	0.114(2)	0.035
$5s_{1/2} \rightarrow 9p_{3/2}$	0.074(2)	0.014
$\alpha_{5s_{1/2}}(c)$		9.3(5)
$\alpha_{5s_{1/2}}(vc)$		-0.26(2)
$\alpha_{5s_{1/2}}(\text{tail})$		0.12(1)
Total		687.3(5)
Expt. [49]		769(61)

the calculated CCSD(T) results, which are slightly larger in magnitude, the polarizability result still does not agree within the experimental error bar. Therefore, it would be instructive to perform another measurement of this dynamic polarizability to assert this result.

It seems from the above analysis that the calculated E1 matrix elements using the CCSD(T) method are reasonably accurate and can be further employed to obtain the polarizabilities of the $5p$ states. However, we can calculate the polarizabilities of the $5p$ states even more precisely if the uncertainties in the dominant contributing E1 matrix elements of the $6s \rightarrow 5p_{1/2,3/2}$, $4d_{3/2} \rightarrow 5p_{1/2,3/2}$, and $4d_{5/2} \rightarrow 5p_{3/2}$ transitions are pushed down further. In order to do so, we evaluate the lifetime of the $6s$ state using our calculated matrix elements as 4.144(3) and 6.048(5) in a.u. of the $6s - 5p_{1/2}$ and $6s - 5p_{3/2}$ transitions, respectively. We obtain its lifetime as 45.44(8) ns against the experimental result of 45.57(17) ns [14] with branching ratios 34% to the $5p_{1/2}$ state and 66% to the $5p_{3/2}$ state, neglecting the observed insignificant transition probabilities to the $5s$ and $4d$ states. Since we are able to obtain a more precise lifetime for the $6s$ state using our calculated matrix elements instead of the measurement, we assume these calculated E1 matrix elements are more precise than what we would have obtained from the known experimental lifetime result.

We would further like to use the above E1 matrix elements to produce the experimental polarizability of the $5p_{1/2}$ state from which we anticipate to estimate the E1 matrix element of the $5p_{1/2} \rightarrow 4d_{3/2}$ transition accurately. Since no direct measurement of the polarizability of the $5p_{1/2}$ state is known to us from the literature, we use the differential polarizability of the $5s \rightarrow 5p_{1/2}$ transition, which is reported as 492.20(7) a.u. [53]. In fact, using the differential polarizability here is advantageous for the following three reasons: (i) we have already determined the polarizability of the $5s$ state precisely, (ii) the differential polarizability is not affected by the uncertainty of the core-correlation contribution, and (iii) precise values of a few important matrix elements contributing towards the $5p$ state polarizability are known to some extent from the above analysis. By adding the experimental differential polarizability with the precisely known polarizability of the $5s$ state, we consider the experimental $5p_{1/2}$ state polarizability as 810.6(6) a.u.; indeed, this result will not meddle the above advantages. We find from our calculations that the E1 matrix elements of the $5p_{1/2} \rightarrow 5s$, $5p_{1/2} \rightarrow 6s$, and $5p_{1/2} \rightarrow 4d_{3/2}$ transitions have crucial contributions to the $5p_{1/2}$ state polarizability. By substituting the precisely known values of the first two elements to reproduce the experimental $5p_{1/2}$ polarizability result, the E1 matrix element of the $5p_{1/2} \rightarrow 4d_{3/2}$ transition is set as 8.069(2) a.u. This agrees well with our calculated result of 8.07(2) a.u. From this analysis, we estimate the theoretical value of the $5p_{1/2}$ state polarizability to be 810.5(1.1) a.u.; contributions from various parts are given explicitly in Table IV.

It can be noticed that the $4d_{5/2}$ state has only one allowed decay channel to the $5p_{3/2}$ state. Therefore, if the lifetime of the $4d_{5/2}$ state is known precisely, then the E1 matrix element of the $5p_{3/2} \rightarrow 4d_{5/2}$ transition can be estimated accurately from this data. There are two experimental results for the lifetime of the $4d_{5/2}$ state reported as 89.5 ns [54] and 94(6) ns [12]. From the former result, which is the latest, we deduce the E1 matrix element of the above transition to be about

TABLE IV. Scalar polarizability of the $5p_{1/2}$ state in Rb (in a.u.). Uncertainties in the results are given in parentheses.

Contribution	E1 amplitude	Contribution to α_v^0
$\alpha_{5p_{1/2}}(v)$		
$5s_{1/2} \rightarrow 5p_{1/2}$	4.227(6)	-103.92(1)
$5p_{1/2} \rightarrow 6s_{1/2}$	4.144(3)	166.32(1)
$5p_{1/2} \rightarrow 7s_{1/2}$	0.962(4)	4.93
$5p_{1/2} \rightarrow 8s_{1/2}$	0.507(3)	1.14
$5p_{1/2} \rightarrow 9s_{1/2}$	0.333(1)	0.452
$5p_{1/2} \rightarrow 10s_{1/2}$	0.235(1)	0.215
$5p_{1/2} \rightarrow 4d_{3/2}$	8.069(2)	702.89(3)
$5p_{1/2} \rightarrow 5d_{3/2}$	1.184(3)	7.816(1)
$5p_{1/2} \rightarrow 6d_{3/2}$	1.002(3)	4.560
$5p_{1/2} \rightarrow 7d_{3/2}$	0.75(2)	2.325(1)
$5p_{1/2} \rightarrow 8d_{3/2}$	0.58(2)	1.320(1)
$5p_{1/2} \rightarrow 9d_{3/2}$	0.45(1)	0.770
$\alpha_{5p_{1/2}}(c)$		9.1(5)
$\alpha_{5p_{1/2}}(vc)$		~ 0.0
$\alpha_{5p_{1/2}}(\text{tail})$		12.6(1.0)
Total		810.5(1.1)

10.89 a.u., which reasonably agrees with our CCSD(T) result of 10.94(6) a.u. The matrix element obtained from the later lifetime data gives a much lower absolute value with very large uncertainty compared to our calculated result, and is not of interest to us. Similarly, the lifetimes of the $4d_{3/2}$ state are reported as 83.4 ns [54] and 86(6) ns [12]. The $4d_{3/2}$ state has two strong allowed decay channels to the $5p_{1/2}$ and $5p_{3/2}$ states. By combining the above E1 matrix element for the $5p_{1/2} \rightarrow 4d_{3/2}$ transition and the lifetime of the $4d_{3/2}$ state as 83.4 ns (the reason for not considering the other value is the same as cited above), we predict the E1 matrix element of the $5p_{3/2} \rightarrow 4d_{3/2}$ transition to be about 3.5 a.u. In order to find this matrix element more precisely, we use the experimental results for the scalar and tensor polarizabilities of the $5p_{3/2}$ state, which are reported as 857(10) and -163(3) in a.u. [55], respectively. Our calculation shows that the major contributions to these polarizabilities come from the matrix elements of the $5p_{3/2} \rightarrow 5s_{1/2}$, $5p_{3/2} \rightarrow 6s_{1/2}$, $5p_{3/2} \rightarrow 4d_{3/2}$, and $5p_{3/2} \rightarrow 4d_{5/2}$ transitions. From the sensitivity in the given precision of the E1 matrix element of the $5p_{3/2} \rightarrow 4d_{3/2}$ transition to be able to reproduce the scalar and tensor polarizabilities in their respective error bars, we get a lower bound for this matrix element of 3.6 a.u. Without any loss of quality, we retain our CCSD(T) result, i.e., 3.65(2) a.u., as the most precise value for this matrix element. Using these optimized results and the combined experimental values of the scalar and tensor polarizabilities of the $5p_{3/2}$ state, we get the best value for the E1 matrix element of the $5p_{3/2} \rightarrow 4d_{5/2}$ transition to be 10.89(1) a.u. After substituting all the above matrix elements, we obtain scalar and tensor static polarizabilities of the $5p_{3/2}$ state as 868.0(1.7) a.u. and -165.9(5) a.u., respectively, which are given with individual contributions in Table V.

Now we list below the optimized E1 matrix elements (in a.u.) obtained from the above analysis apart from our

TABLE V. Scalar and tensor polarizabilities of the $5p_{3/2}$ state in Rb (in a.u.). Uncertainties in the results are given in parentheses.

Contribution	E1 amplitude	α_v^0	α_v^2
$\alpha_{5p_{1/2}}(v)$			
$5p_{3/2} \rightarrow 5s_{1/2}$	5.977(9)	-101.96(2)	101.96(2)
$5p_{3/2} \rightarrow 6s_{1/2}$	6.048(5)	182.89(2)	-182.89(2)
$5p_{3/2} \rightarrow 7s_{1/2}$	1.363(4)	5.036	-5.036
$5p_{3/2} \rightarrow 8s_{1/2}$	0.714(3)	1.149	-1.149
$5p_{3/2} \rightarrow 9s_{1/2}$	0.468(2)	0.453	-0.453
$5p_{3/2} \rightarrow 10s_{1/2}$	0.330(2)	0.215	-0.215
$5p_{3/2} \rightarrow 4d_{3/2}$	3.65(2)	74.52(1)	59.62(1)
$5p_{3/2} \rightarrow 5d_{3/2}$	0.59(2)	0.988	0.791
$5p_{3/2} \rightarrow 6d_{3/2}$	0.48(2)	0.531	0.425
$5p_{3/2} \rightarrow 7d_{3/2}$	0.355(4)	0.264	0.211
$5p_{3/2} \rightarrow 8d_{3/2}$	0.272(3)	0.147	0.118
$5p_{3/2} \rightarrow 9d_{3/2}$	0.212(2)	0.086	0.069
$5p_{3/2} \rightarrow 4d_{5/2}$	10.89(1)	663.4(5)	-132.7(1)
$5p_{3/2} \rightarrow 5d_{5/2}$	1.76(3)	8.792(5)	-1.758(1)
$5p_{3/2} \rightarrow 6d_{5/2}$	1.42(3)	4.647(3)	-0.929(1)
$5p_{3/2} \rightarrow 7d_{5/2}$	1.06(2)	2.353(1)	-0.471
$5p_{3/2} \rightarrow 8d_{5/2}$	0.81(1)	1.304	-0.261
$5p_{3/2} \rightarrow 9d_{5/2}$	0.593(5)	0.677	-0.135
$\alpha_{5p_{3/2}}(c)$		9.1(5)	0.0
$\alpha_{5p_{3/2}}(vc)$		~ 0.0	~ 0.0
$\alpha_{5p_{3/2}}(\text{tail})$		13.40(1.5)	-3.15(50)
Total		868.0(1.7)	-165.9(5)

calculated results as

$$\begin{aligned}
 \langle 5s || D || 5p_{1/2} \rangle &= 4.227(6), \\
 \langle 5s || D || 5p_{3/2} \rangle &= 5.977(9), \\
 \langle 5p_{1/2} || D || 4d_{3/2} \rangle &= 8.069(2), \\
 \langle 5p_{3/2} || D || 4d_{5/2} \rangle &= 10.89(1).
 \end{aligned} \tag{19}$$

B. Lifetimes of few excited states

Since we are now able to estimate some of the E1 matrix elements more precisely than the previously known results, we would like to use them further to estimate the lifetimes of the first few excited states in the Rb atom accurately. The matrix elements for the $\langle 5s || D || 5p_{1/2} \rangle$ and $\langle 5s || D || 5p_{3/2} \rangle$ transitions were obtained from the lifetime measurements, so we still consider the most accurately known lifetimes of the $5p_{1/2}$ and $5p_{3/2}$ states from the experiment as 27.75(8) and 26.25(8) ns, respectively. We now determine the lifetimes of the $4d$ and $6s$ states using the E1 matrix elements listed in Eq. (19) and from our calculations, which are given in Table I. The estimated lifetimes are mentioned in Table VI as recommended

TABLE VI. Comparison of lifetimes (in ns) of three excited states in the Rb atom from various theoretical and experimental studies.

Level	Recommended	Other theory [18]	Expt.
$4d_{3/2}$	82.30(17)	83.0(8)	86(6) [12]
$4d_{5/2}$	89.32(16)	89.4(9)	94(6) [12]
$6s_{1/2}$	45.44(8)	45.4(1)	45.57(17) [14]

values and compared with the other available experimental and theoretical results in the same table.

C. Status of the polarizability results

To affirm the broad interest of studying polarizabilities in the Rb atom, we discuss briefly below the various experimental and theoretical works in the evaluation of polarizabilities of the $5s$ and $5p$ states reported so far in the Rb atom. There were several measurements carried out on Stark shifts in the Rb atom almost two decades ago [53,60–62] from which the polarizabilities of the $5s$ ground state and few excited states were estimated. Hunter and coworkers had observed the dc Stark shifts of the D_1 line in Rb using a pair of cavity stabilized diode lasers locked to resonance signals [53,60,61]. In another work, Tanner and Wieman had used crossed-beam laser spectroscopy with frequency stabilized laser diodes to measure the differential Stark shift of the D_2 line [62]. Marrus *et al.* had used an atomic beam method long ago to measure the Stark shift from which both the scalar and tensor polarizabilities of the $5p_{3/2}$ state were determined [63].

The extensive calculation of polarizabilities in the Rb atom was carried out by Marinescu *et al.* using an l -dependent model potential [46]. In this work, the infinite second-order sums in the polarizability calculations were transformed into integrals over the solutions of two coupled inhomogeneous differential equations and the integrals were carried out using the Numerov integration method [64]. In 2004, Zhu *et al.* employed the RCC method to calculate the scalar and tensor polarizabilities of the ground and the first p excited states in alkali atoms [47]. The results obtained using the RCC method were substantially improved over the earlier calculations based on the nonrelativistic theories. Later, Arora *et al.* extended these calculations to obtain frequency-dependent scalar and tensor polarizabilities of the ground and first excited $5p$ states in Rb [31,48,65] using the RCC method at the linearized single, double, and partial triple excitations level (SDpT method).

As discussed earlier, we have optimized at least seven important E1 matrix elements, which are crucial in obtaining the polarizabilities of the $5s$ and $5p$ states, and the other matrix elements have been obtained using the CCSD(T) method, which includes all of the nonlinear terms. Therefore, the predicted polarizabilities of the $5s$ and $5p$ states obtained in this work are expected to be accurate enough to employ them further in the determination of the magic wavelengths in the Rb atom, which is the prime motivation of the present work. In Table VII, we compare our polarizability results with the other reported values. Our results are more accurate than the earlier studied results mainly due to the optimization of the matrix elements.

To the best of our knowledge, there are no experimental and/or theoretical results on vector polarizabilities of the $5s$ and $5p$ states for any wavelengths available in the Rb atom to compare with the present calculations. Accuracy in these polarizabilities will determine the correct values of the magic wavelengths for the circularly polarized light in this atom. Since the E1 matrix elements required to determine the vector polarizabilities are the same as those required for the calculation of scalar and tensor polarizabilities, we expect a similar precision in our used vector polarizability results, as discussed below. We shall present the vector polarizabilities

TABLE VII. Comparison of the static and ac polarizabilities (in a.u.) in the Rb atom for the $5s$, $5p_{1/2}$, and $5p_{3/2}$ states with other experiments and theory.

	α_{5s}^0	$\alpha_{5p_{1/2}}^0$	$\alpha_{5p_{3/2}}^0$	$\alpha_{5p_{3/2}}^2$
Present	318.3(6)	810.5(1.1)	868.0(1.7)	-165.9(5)
Other	317.39 [56]	805 [31]	867 [31]	-167 [31]
Other	318.6(6) [57]	807 [58]	870 [58]	-171 [58]
Expt.	318.79(1.42) [51]	810.6(6) [53,59]	857(10) [55]	-163(3) [55]

in the $5s$ and $5p$ states at a given wavelength (say close to a particular λ_{magic} value) so that if necessary our results can also be further verified by any other study.

D. AC Stark shifts and magic wavelengths

Following Eq. (6), the ac Stark shift ΔE_v of an atomic-energy level E_v due to the external applied ac electric field \mathcal{E} , in the absence of any magnetic field, can be parametrized in terms of α_0 , α_1 , and α_2 as [32]

$$\Delta E_v = -\frac{1}{2}\mathcal{E}^2 \left\{ \alpha_v^0(\omega) + \mathcal{A} \frac{m_j}{j_v} \alpha_v^1(\omega) + \left[\frac{3m_j^2 - j_v(j_v + 1)}{j_v(2j_v - 1)} \right] \alpha_v^2(\omega) \right\}. \quad (20)$$

In this formula, the frequency ω is assumed to be several linewidths off-resonance. The differential ac Stark shift for a transition is defined as the difference between the Stark shifts of individual levels. For instance, the interested differential ac Stark shifts in our case are for the $5p_i-5s$ transitions (with $i = 1/2, 3/2$), which are given by

$$\begin{aligned} \delta(\Delta E)_{5p_i-5s} &= \Delta E_{5p_i} - \Delta E_{5s} \\ &= \frac{1}{2}\mathcal{E}^2(\alpha_{5s} - \alpha_{5p_i}), \end{aligned} \quad (21)$$

where we have used the total polarizabilities of the respective states. Since the external electric field \mathcal{E} is arbitrary, we can verify the frequencies or wavelengths where $\alpha_{5p_i} = \alpha_{5s}$ for the null differential ac Stark shifts.

In order to estimate the total polarizability for any particular set of j_v and m_j values, we need to determine the scalar, vector, and tensor polarizabilities. Magic wavelengths are calculated for continuous values of frequencies (and can also be expressed in terms of wavelength λ) by plotting the total polarizability for different states against the λ values. The crossing between the two polarizabilities at various values of wavelengths will correspond to λ_{magic} . Trapping of Rb atoms is convenient at these wavelengths, as was stated in the beginning. As pointed out in Ref. [31], the linearly polarized lattice scheme offers only a few cases in which the magic wavelengths are suitable from the experimental point of view. Therefore, we would like to explore the idea of using the circularly polarized light for which the magic wavelengths need to be determined separately for each magnetic quantum number m_j .

In the next two sections, we shall discuss the magic wavelengths for the $5p_{1/2,3/2}-5s$ transitions for both the linearly and circularly polarized lights. The reason for bringing up the issue of magic wavelengths for the linearly polarized lights in these transitions is that since we have obtained the most accurate results for all of the static polarizabilities, it is expected that

we will get better results for the magic wavelengths using our optimized set of E1 matrix elements. This will also help us to make a comparison study between the results obtained from the linearly and circularly polarized lights.

E. Case for the linearly polarized optical traps

Since we are interested in optical traps and the previous study [31] reveals that the magic wavelengths for the $5s-5p$ transitions at which the Rb atom can be trapped using the linearly polarized lights lie between 600–1500 nm, we try to find out the null differential polarizabilities in this region. In Fig. 1, we plot the total polarizabilities due to the linearly polarized lights for both the $5s$ and $5p_{1/2}$ states. As seen in the figure, the $5s$ state dynamic polarizabilities are generally small in this region, except for the wavelengths in close vicinity to the $5s-5p_{1/2}$ resonance (at 795 nm) and the $5s-5p_{3/2}$ resonance (at 780 nm). However, the $5p_{1/2}$ state has several resonances in the considered wavelength range. It is generally expected that the $5p_{1/2}$ state polarizability will cross the $5s$ state polarizability in between each pair of resonances. We found a total of six magic wavelengths for the $5p_{1/2} \rightarrow 5s$ transition in between the five resonances.

However, the case for the $5p_{3/2} \rightarrow 5s$ transition is different owing to the presence of the nonzero tensor contribution of the $5p_{3/2}$ state. As shown in Fig. 2, we get different magic wavelengths for the $5p_{3/2} \rightarrow 5s$ transition at the $m_j = \pm 1/2$ and $m_j = \pm 3/2$ sublevels of the $5p_{3/2}$ state. There are few wavelengths in between resonances where $\alpha_{5p_{3/2}}$ with the $m_j = \pm 3/2$ contribution is not the same as the α_{5s} . This leads to a reduction in the number of magic wavelengths for this

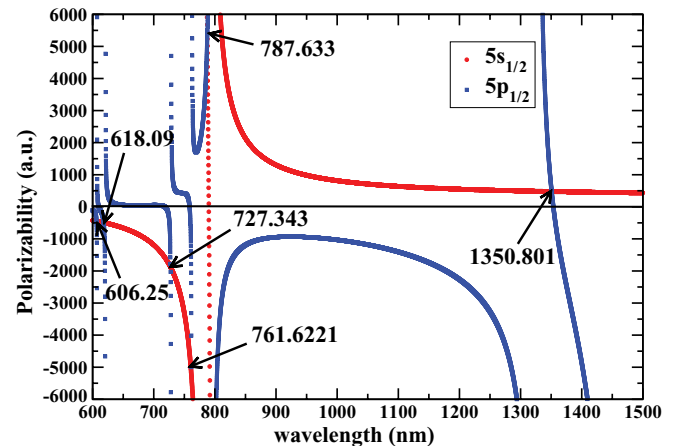


FIG. 1. (Color online) Magic wavelengths identified by arrows for the $5p_{1/2}-5s$ transition in Rb using the linearly polarized light.

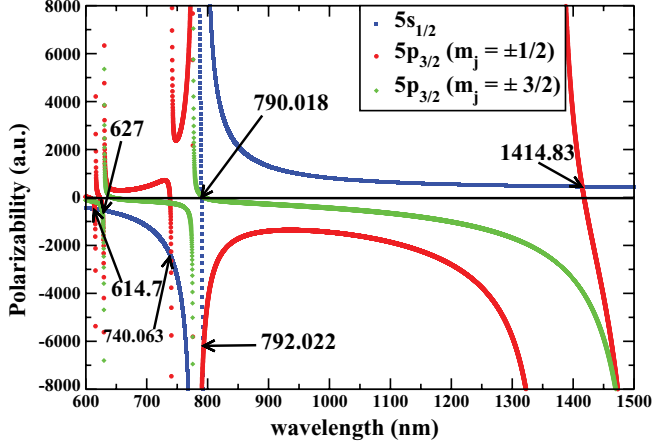


FIG. 2. (Color online) Magic wavelengths identified by arrows for the $5p_{3/2}$ - $5s$ transition in Rb using the linearly polarized light.

transition. For example, we did not find any λ_{magic} between the $5p_{3/2}$ - $4d_{3/2,5/2}$ resonances (at 1529 nm) and the $5p_{3/2}$ - $6s$ resonance (at 1367 nm) for $m_j = \pm 3/2$ sublevels of the $5p_{3/2}$ state.

We have limited our search for the magic wavelengths where the differential polarizabilities between the $5s$ and $5p_j$ states are less than 0.5%. Based on all of this data, we list now λ_{magic} (in vacuum) above 600 nm in Table VIII for the $5p_{1/2}$ - $5s$ and $5p_{3/2}$ - $5s$ transitions in the Rb atom and compare them with the previously known results. The present results are improved slightly due to the optimized E1 matrix elements used here. The uncertainties in our magic wavelength results are found as the maximum differences between the $\alpha_{5s} \pm \delta\alpha_{5s}$ and $\alpha_{5p} \pm \delta\alpha_{5p}$ contributions with their respective magnetic

TABLE VIII. Magic wavelengths λ_{magic} for the linearly polarized light above 600 nm for the $5p_{1/2}$ - $5s$ and $5p_{3/2}$ - $5s$ transitions in Rb and the corresponding values of polarizabilities at the magic wavelengths. The wavelengths (in vacuum) are given in nm and the polarizabilities are given in a.u. The given m_j values correspond to the $5p$ states.

$ m_j $	λ_{magic}	λ_{magic} [31]	$\alpha(\lambda_{\text{magic}})$
Transition: $5p_{1/2}$ - $5s$			
1/2	606.25(1)	606.2(1)	-443.3
1/2	618.09(2)	617.7(7)	-490
1/2	727.343(2)	727.35(1)	-1876
1/2	761.6221(2)	761.5(1)	-5270
1/2	787.633(2)	787.6(1)	5382
1/2	1350.801(9)	1350.9(5)	475.5
Transition: $5p_{3/2}$ - $5s$			
1/2	614.70(1)	614.7(1)	-477
3/2	626.62(3)	626.2(9)	-529
1/2	627.70(1)	627.3(5)	-534
1/2	740.063(2)	740.07(1)	-2493
1/2	775.868(1)	775.84(1)	-20030
3/2	775.8228(2)	775.77(3)	-19917
3/2	790.018(2)	789.98(2)	53
1/2	792.022(1)	792.00(1)	-6973
1/2	1414.83(3)	1414.8(5)	455

quantum numbers, where the $\delta\alpha$ are the uncertainties in the polarizabilities for their corresponding states.

The reason for not acquiring a sufficient number of magic wavelengths for the $5p_{3/2}$ - $5s$ transition lies in the fact that the extra contribution from the tensor polarizability to the total $5p_{3/2}$ polarizability is not compensated by the counterpart of the $5s$ state. The idea of using the circularly polarized light to obtain magic wavelengths for the $5p_{3/2}$ - $5s$ transition is triggered by that fact that the extra contribution from the tensor polarizability to the $5p_{3/2}$ state might be canceled by the vector polarizability contributions, or the vector polarizabilities are so large that they may play a dominant role in determining the differential polarizabilities. This would be evident in the following section.

F. Case for the circularly polarized optical traps

As mentioned previously, polarizabilities for the circularly polarized light have an extra contribution from the vector component of the tensor product between the dipole operators. This extra factor is expected to provide better results for state-insensitive trapping. First, we present the scalar, vector, and tensor dynamic polarizabilities of the $5s$, $5p_{1/2}$, and $5p_{3/2}$ states in Tables IX, X, and XI, respectively, at $\lambda = 770$ nm to perceive their general behavior. The choice of this wavelength is deliberate since it is close to one of the magic wavelengths for the circularly polarized light (e.g., see Tables XII and XIII). Hereafter we shall consider the left-handed circularly polarized light for all practical purposes, as the results will have a similar trend with the right-handed circularly polarized light due to the linear dependency of the degree of polarizability \mathcal{A} in Eq. (20). Nevertheless, the left- or right-handed polarization in the experimental setup is just a matter of choice.

For the sake of the completeness of our study, we also search for magic wavelengths in the $5s$ - $5p_{1/2}$ transition in Rb atoms using the circularly polarized light, although a fairly large number of magic wavelengths for this transition is found using the linearly polarized light. For this purpose,

TABLE IX. Contributions to the $5s$ scalar (α_v^0) and vector (α_v^1) polarizabilities at $\lambda = 770$ nm in Rb. Uncertainties in the results are given in parentheses.

Contribution	α_v^0	α_v^1
$\alpha_{5s_{1/2}}(v)$		
$5s_{1/2} \rightarrow 5p_{1/2}$	-1576.1(2)	3254.4(4)
$5s_{1/2} \rightarrow 6p_{1/2}$	0.515	-0.565
$5s_{1/2} \rightarrow 7p_{1/2}$	0.047	0.044
$5s_{1/2} \rightarrow 8p_{1/2}$	0.011	0.010
$5s_{1/2} \rightarrow 9p_{1/2}$	0.006	0.005
$\alpha_{5s_{1/2}}(c)$		
$5s_{1/2} \rightarrow 5p_{3/2}$	-7615(1)	-7716(1)
$5s_{1/2} \rightarrow 6p_{3/2}$	1.339	0.731
$5s_{1/2} \rightarrow 7p_{3/2}$	0.144	0.067
$5s_{1/2} \rightarrow 8p_{3/2}$	0.039	0.017
$5s_{1/2} \rightarrow 9p_{3/2}$	0.016	0.007
$\alpha_{5s_{1/2}}(vc)$		
$\alpha_{5s_{1/2}}(vc)$	-0.26(2)	~0.0
α_{tail}	0.14(1)	0.002(1)
Total	-9180(1.1)	-4462(1.1)

TABLE X. Contributions to the $5p_{1/2}$ scalar (α_v^0) and vector (α_v^1) polarizabilities at $\lambda = 770$ nm in Rb. Uncertainties in the results are given in parentheses.

Contribution	α_v^0	α_v^1
$\alpha_{5p_{1/2}}(v)$		
$5p_{1/2} \rightarrow 5p_{1/2}$	1567.1(2)	3254.4(4)
$5p_{1/2} \rightarrow 6s_{1/2}$	-85.029(5)	292.38(2)
$5p_{1/2} \rightarrow 7s_{1/2}$	46.676(4)	-88.283(7)
$5p_{1/2} \rightarrow 8s_{1/2}$	3.020	-4.764
$5p_{1/2} \rightarrow 9s_{1/2}$	0.954	-1.382
$5p_{1/2} \rightarrow 10s_{1/2}$	0.412	-0.570
$5p_{1/2} \rightarrow 4d_{3/2}$	-262.99(1)	-504.00(2)
$5p_{1/2} \rightarrow 5d_{3/2}$	382.94(2)	379.02(2)
$5p_{1/2} \rightarrow 6d_{3/2}$	13.029(1)	10.504(1)
$5p_{1/2} \rightarrow 7d_{3/2}$	5.035(2)	3.694(2)
$5p_{1/2} \rightarrow 8d_{3/2}$	2.565(1)	1.787(1)
$5p_{1/2} \rightarrow 9d_{3/2}$	1.413	0.954
$\alpha_{5p_{1/2}}(c)$	9.2(5)	0.0
$\alpha_{5p_{1/2}}(vc)$	~ 0.0	~ 0.0
α_{tail}	17.6(20)	3.8(4)
Total	1711(2)	3347.7(4)

we plot the net dynamic polarizability results of the $5s$ and $5p_{1/2}$ states in Fig. 3 using the circularly polarized light against different values of wavelength. The figure shows that the total polarizability of the $5s$ state for any values of λ is very small, except for the wavelengths close to the two

TABLE XI. Contributions to the $5p_{3/2}$ scalar (α_v^0), vector (α_v^1), and tensor (α_v^2) polarizabilities at $\lambda = 770$ nm in Rb. Uncertainties in the results are given in parentheses.

Contribution	α_v^0	α_v^1	α_v^2
$\alpha_{5p_{3/2}}(v)$			
$5p_{3/2} \rightarrow 5s_{1/2}$	3807.5(7)	11575(2)	-3807.5(7)
$5p_{3/2} \rightarrow 6s_{1/2}$	-85.017(9)	452.76(5)	85.017(9)
$5p_{3/2} \rightarrow 7s_{1/2}$	68.181(6)	-196.85(2)	-68.181(6)
$5p_{3/2} \rightarrow 8s_{1/2}$	3.194	-7.667(1)	-3.194
$5p_{3/2} \rightarrow 9s_{1/2}$	0.984	-2.168	-0.984
$5p_{3/2} \rightarrow 10s_{1/2}$	0.422	-0.885	-0.422
$5p_{3/2} \rightarrow 4d_{3/2}$	-25.311(5)	60.32(1)	-20.249(4)
$5p_{3/2} \rightarrow 5d_{3/2}$	-61.57(1)	74.47(1)	-49.25(1)
$5p_{3/2} \rightarrow 6d_{3/2}$	1.607(1)	-1.578(1)	1.286(1)
$5p_{3/2} \rightarrow 7d_{3/2}$	0.591	-0.527	0.473
$5p_{3/2} \rightarrow 8d_{3/2}$	0.293	-0.248	0.234
$5p_{3/2} \rightarrow 9d_{3/2}$	0.162	-0.133	0.130
$5p_{3/2} \rightarrow 4d_{5/2}$	-225.3(2)	-805.4(6)	45.06(4)
$5p_{3/2} \rightarrow 5d_{5/2}$	-564.1(3)	-1023.3(6)	112.8(1)
$5p_{3/2} \rightarrow 6d_{5/2}$	14.06(1)	20.70(1)	-2.811(2)
$5p_{3/2} \rightarrow 7d_{5/2}$	5.264(2)	7.046(3)	-1.053
$5p_{3/2} \rightarrow 8d_{5/2}$	2.597(1)	3.298(1)	-0.519
$5p_{3/2} \rightarrow 9d_{5/2}$	1.2700	1.562	-0.254
$\alpha_{5p_{3/2}}(c)$	9.3(5)	0.0	0.0
$\alpha_{5p_{3/2}}(vc)$	~ 0.0	~ 0.0	~ 0.0
α_{tail}	19(2)	6.9(7)	-4.7(9)
Total	2973(2)	10163(5)	-3714(1)

TABLE XII. Magic wavelengths λ_{magic} above 600 nm for the $5p_{1/2}-5s$ transition in Rb and the corresponding values of total polarizabilities at the magic wavelengths for the left-handed circularly polarized laser beam. The wavelengths (in vacuum) are given in nm and polarizabilities are given in a.u. The given m_j values are for the $5p$ states.

m_j	λ_{magic}	$\alpha(\lambda_{\text{magic}})$	λ_{magic} (avg)
Transition: $5p_{1/2}-5s$			
1/2	600.83(14)	-405	
-1/2	607.98(1)	-428	604(7)
-1/2	616.77(2)	-461	617
1/2	721.628(23)	-1449	
-1/2	728.843(1)	-1633	725(7)
-1/2	761.176(1)	-3424	761
-1/2	1306.08(1)	504	1306

primary resonances. Due to the m_j dependence of the vector polarizability coefficient in Eq. (20), the crossing occurs at a different wavelength for the different values of m_j in between two $5p_{1/2}$ resonances. As shown in Table XII, we get a set of five magic wavelengths in between seven $5p_{1/2}$ resonances lying in the wavelength range 600–1400 nm. Out of these five sets of magic wavelengths, three sets occur only for negative values of m_j . Thus, the number of convenient magic wavelengths for the above transition is less than the number of magic wavelengths obtained for the linearly polarized light.

TABLE XIII. Magic wavelengths λ_{magic} above 600 nm for the $5p_{3/2}-5s$ transition in Rb and the corresponding values of total polarizabilities at the magic wavelengths for the left-handed circularly polarized laser beam. The wavelengths (in vacuum) are given in nm and polarizabilities are given in a.u. The given m_j values are for the $5p$ states.

m_j	λ_{magic}	$\alpha(\lambda_{\text{magic}})$	λ_{magic} (avg)
Transition: $5p_{3/2}-5s$			
1/2	613.25(3)	-447	
-1/2	615.51(1)	-456	616(5)
-3/2	618.15(2)	-466	
3/2	630.142(1)	-516	
1/2	628.30(1)	-508	
-1/2	626.95(1)	-502	628(5)
-3/2	625.04(3)	-494	
3/2	746.737(15)	-2328	
1/2	738.794(32)	-1964	
-1/2	740.587(1)	-2037	742(8)
-3/2	742.262(1)	-2109	
3/2	775.836(5)	-6231	
1/2	775.834(7)	-6230	
-1/2	775.789(3)	-6215	775.8(2)
-3/2	775.693(2)	-6183	
1/2	783.883(13)	-10925	
-1/2	787.547(4)	-16431	786(4)
-3/2	776.497(4)	-16318	
1/2	1454.4(9)	453	
-1/2	1387.1(1)	473	1382(149)
-3/2	1305.9(1)	504	

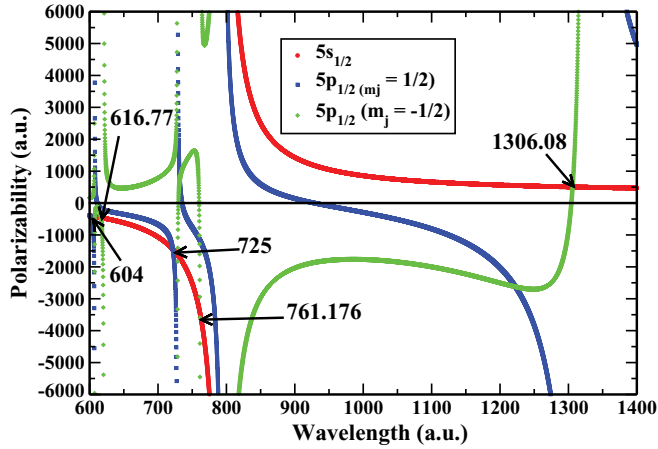


FIG. 3. (Color online) Magic wavelengths identified by arrows for the $5p_{1/2}$ - $5s$ transition in Rb using the left-handed circularly polarized light.

This advocates for the use of linearly polarized light in this transition, although the choice of the circularly polarized light is not bad at all. The m_j dependence of traps and the difficulties in building a viable experimental setup in the case of circularly polarized light could be the other major concern.

In this work, we also propose the use of the “switching trapping scheme” (described below), which may solve the problem in cases where state-insensitive trapping is only supportive for the negative m_j sublevels of $5p$ states. We observed that the same magic wavelength will support state-insensitive trapping for negative m_j sublevels if we switch the sign of \mathcal{A} and m_j of the $5s$ state. In other words, the change of sign of \mathcal{A} and m_j sublevels of the $5s$ state will lead to the same result for the positive values of m_j sublevels of $5p$ states.

Here we give more emphasis on finding more magic wavelengths for the $5s$ - $5p_{3/2}$ transition, which can be used in the state-insensitive trapping scheme for the Rb atom. In Table XIII, we list a number of λ_{magic} for the $5s$ - $5p_{3/2}$ transition in the far-optical and near-infrared wavelengths, along with the uncertainties in the λ_{magic} and the polarizabilities at the λ_{magic} values. We also list the $\lambda_{\text{magic}}(\text{avg})$ values in the table, which are the average of the magic wavelengths at different m_j sublevels. The error in the $\lambda_{\text{magic}}(\text{avg})$ is calculated as the maximum difference between the magic wavelengths from different m_j sublevels. For this transition, we get a set of six magic wavelengths in between seven $5p_{3/2}$ resonances lying in the wavelength range 600–1400 nm (i.e., $5p_{3/2}$ - $4d_j$ resonance at 1529 nm, $5p_{3/2}$ - $6s$ resonance at 1367 nm, $5p_{3/2}$ - $5s$ resonance at 780 nm, $5p_{3/2}$ - $5d_j$ resonance at 776 nm, $5p_{3/2}$ - $7s$ resonance at 741 nm, $5p_{3/2}$ - $6d_j$ resonance at 630 nm, and $5p_{3/2}$ - $8s$ resonance at 616 nm). Five out of six magic wavelengths support a blue-detuned trap (predicted by the negative values of dynamic polarizability). Out of these five magic wavelengths, the magic wavelengths at 628 and 742 nm are recommended for blue-detuned traps. The magic wavelength at 742 nm supports a stronger trap [as shown by a larger value of the polarizability at this wavelength in Fig. (4)]. The magic wavelength at 775.8 nm is very close to the resonance and might not be useful for practical purposes. The magic wavelength at 1382 nm supports a red-detuned

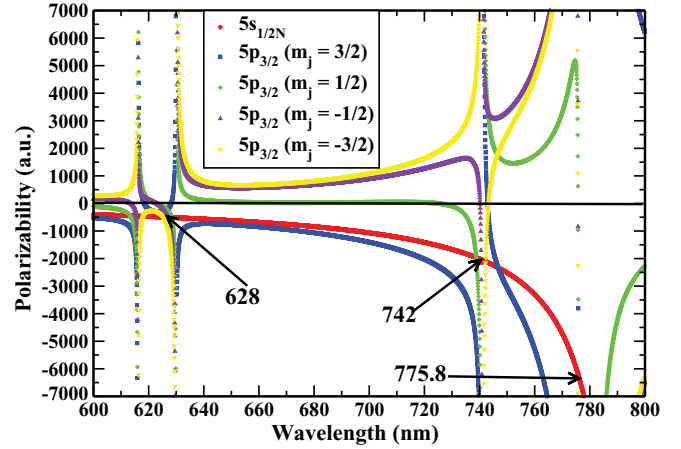


FIG. 4. (Color online) Magic wavelengths identified by arrows for the $5p_{3/2}$ - $5s$ transition in Rb using the left-handed circularly polarized light.

optical trap. It can be observed from Table XIII that the $m_j = 3/2$ sublevel does not support state-insensitive trapping at this wavelength. However, the use of a switching trapping scheme, as described in the previous paragraph, will allow trapping this sublevel too. The magic wavelength at 1382 nm is recommended owing to the fact that it is not close to any atomic resonance and supports a red-detuned trap, which was not found in the linearly polarized trapping scheme.

V. SUMMARY

In conclusion, we have employed the relativistic coupled-cluster method to the single and double excitations and the triples excitation approximation to determine the electric dipole matrix elements in rubidium atom. Some of the important matrix elements were further optimized using the experimental lifetimes of few excited states, and static polarizabilities of the ground and $5p_{1/2,3/2}$ excited states. These optimized matrix elements were then used to improve the precision of the available lifetime results for some of the low-lying excited states in the considered atom. We also observed disagreement between our calculated dynamic polarizability with a measurement at the wavelength 1064 nm using the above optimized matrix elements.

We have compared the static and dynamic polarizability results from various works and reported the improved values of the magic wavelengths for the $5s \rightarrow 5p_{1/2}$ transition using the linearly polarized light. Issues related to state-insensitive trapping of rubidium atoms for the $5s \rightarrow 5p_{3/2}$ transition with linearly polarized light are discussed and use of the circularly polarized light is emphasized. Finally, we evaluate six sets of magic wavelengths for the $5s \rightarrow 5p_{3/2}$ transition, which can be used for the above purpose, out of which we have recommended two magic wavelengths at 628 and 742 nm for the blue-detuned optical traps and 1382 nm for the red-detuned optical traps. We also proposed the use of a switching trapping scheme for the magic wavelengths at which the state-insensitive trapping is supported only for either positive or negative m_j sublevels of $5p$ states.

ACKNOWLEDGMENTS

B.K.S. thanks D. Nandy for his help in this work. The work of B.A. was supported by the Department of Science and

Technology, India. Computations were carried out using the 3TFLOP HPC Cluster at the Physical Research Laboratory, Ahmedabad.

-
- [1] A. Godone, F. Levi, S. Micalizio, E. K. Bertacco, and C. E. Calosso, *IEEE Trans. Instrum. Meas.* **56**, 378 (2007).
- [2] J. Vanier and C. Mandache, *Appl. Phys. B* **87**, 565 (2007).
- [3] B. Butscher, J. Nipper, J. B. Balewski, L. Kukota, V. Bendkowsky, R. Low, and T. Pfau, *Nature Phys.* **6**, 970 (2012).
- [4] X. L. Zhang, L. Isenhower, A. T. Gill, T. G. Walker, and M. Saffman, *Phys. Rev. A* **82**, 030306 (2010).
- [5] Y. O. Dudin, A. G. Radnaev, R. Zhao, J. Z. Blumoff, T. A. B. Kennedy, and A. Kuzmich, *Phys. Rev. Lett.* **105**, 260502 (2010).
- [6] S. Tassy, N. Nemitz, F. Baumer, C. Hohl, A. Batar, and A. Gorlitz, *J. Phys. B* **43**, 205309 (2010).
- [7] J. Guena, P. Rosenbusch, P. Laurent, M. Abgrall, D. Rovera, G. Santarellu, M. E. Tobar, S. Bize, and A. Clairon, *IEEE Trans. Ultrason. Ferroelec. Freq. Control* **57**, 647 (2010).
- [8] H. Marion, F. Pereira dos Santos, M. Abgrall, S. Zhang, Y. Sortais, S. Bize, I. Maksimovic, D. Calonico, J. Gruenert, C. Mandache, P. Lemonde, G. Santarelli, P. Laurent, A. Clairon, and C. Salomon, *Phys. Rev. Lett.* **90**, 150801 (2003).
- [9] International Committee for Weights and Measures, Proceedings of the Sessions of the 95th Meeting, October 2006 (unpublished), <http://www.bipm.org/utills/en/pdf/CIPM2006-EN.pdf>.
- [10] D. Sheng, L. A. Orozco, and E. Gomez, *J. Phys. B* **43**, 074004 (2010).
- [11] H. S. Nataraj, B. K. Sahoo, B. P. Das, and D. Mukherjee, *Phys. Rev. Lett.* **101**, 033002 (2008).
- [12] C. E. Theodosiou, *Phys. Rev. A* **30**, 2881 (1984).
- [13] W. A. van Wijngaarden and J. Sagle, *Phys. Rev. A* **45**, 1502 (1992).
- [14] E. Gomez, F. Baumer, A. D. Lange, G. D. Sprouse, and L. A. Orozco, *Phys. Rev. A* **72**, 012502 (2005).
- [15] D. Sheng, A. Perez Galvan, and L. A. Orozco, *Phys. Rev. A* **78**, 062506 (2008).
- [16] J. Marek and P. Munster, *J. Phys. B* **13**, 1731 (1980).
- [17] C. Tai, W. Happer, and R. Gupta, *Phys. Rev. A* **12**, 736 (1975).
- [18] M. S. Safronova and U. I. Safronova, *Phys. Rev. A* **83**, 052508 (2011).
- [19] J. Walls, J. Clarke, S. Cauchi, G. Karkas, H. Chen, and W. A. van Wijngaarden, *Eur. Phys. J. D* **14**, 9 (2001).
- [20] H.-C. Chui, M.-S. Ko., Y.-W. Liu, J.-T. Shy, J.-L. Peng, and H. Ahn, *Opt. Lett.* **30**, 842 (2005).
- [21] A. P. calvan calvan, Y. Zhaoa, L. A. Orozco, E. Gomez, A. D. Lange, F. Baumer, and G. D. Sprouse, *Phys. Lett. B* **655**, 114 (2007).
- [22] N. Schlosser, G. Reymond, I. Protsenko, and P. Grangier, *Nature (London)* **411**, 1024 (2001).
- [23] S. Kuhr, W. Alt, D. Schrader, M. Muller, V. Gomer, and D. Meschede, *Science* **293**, 278 (2001).
- [24] H. Katori, in *Proceedings of the Sixth Symposium on Frequency Standards and Metrology*, edited by P. Gill (World Scientific, Singapore, 2002), pp. 323–330.
- [25] C. A. Sackett, D. Kielpinski, B. E. King, C. Langer, V. Meyer, C. J. Myatt, M. Rowe, Q. A. Turchette, W. M. Itano, D. J. Wineland *et al.*, *Nature (London)* **404**, 256 (2000).
- [26] M. S. Safronova, C. J. Williams, and C. W. Clark, *Phys. Rev. A* **67**, 040303(R) (2003).
- [27] M. Takamoto and H. Katori, *Phys. Rev. Lett.* **91**, 223001 (2003).
- [28] H. Katori, T. Ido, and M. Kuwata-Gonokami, *J. Phys. Soc. Jpn.* **68**, 2479 (1999).
- [29] A. D. Ludlow *et al.*, *Science* **319**, 1805 (2005).
- [30] J. McKeever, J. R. Buck, A. D. Boozer, A. Kuzmich, H.-C. Nagerl, D. M. Stamper-Kurn, and H. J. Kimble, *Phys. Rev. Lett.* **90**, 133602 (2003).
- [31] B. Arora, M. S. Safronova, and C. W. Clark, *Phys. Rev. A* **76**, 052509 (2007).
- [32] V. V. Flambaum, V. A. Dzuba, and A. Derevianko, *Phys. Rev. Lett.* **101**, 220801 (2008).
- [33] C. Y. Park, H. Noh, C. M. Lee, and D. Cho, *Phys. Rev. A* **63**, 032512 (2001).
- [34] K. D. Bonin and V. V. Kresin, *Electric-dipole Polarizabilities of Atoms, Molecules and Clusters* (World Scientific, Singapore, 1997).
- [35] N. L. Manakov, V. D. Ovsiannikov, and L. P. Rapoport, *Phys. Rep.* **141**, 319 (1986).
- [36] I. Lindgren, *Int. J. Quantum Chem.* **12**, 33 (1978).
- [37] B. K. Sahoo, B. P. Das, R. K. Chaudhuri, and D. Mukherjee, *J. Comput. Methods Sci. Eng.* **7**, 57 (2007).
- [38] B. Arora, D. Nandy, and B. K. Sahoo, *Phys. Rev. A* **85**, 012506 (2012).
- [39] C. E. Moore, *Atomic Energy Levels*, Natl. Bur. Stand. Ref. Data Ser. (US GPO, Washington, D.C., 1971), Vol. 35.
- [40] Y. Ralchenko, F. C. Jou, D. E. Kelleher, A. E. Kramida, A. Musgrove, J. Reader, W. L. Wiese, and K. Olsen, *NIST Atomic Spectra Database* (2005) (version 3.1.2) (Nat. Inst. Stand. Technol., Gaithersburg, MD, 2007), <http://physics.nist.gov/asd3>.
- [41] J. Sansonetti, W. Martin, and S. Young, *Handbook of Basic Atomic Spectroscopic Data* (version 1.1.2) (Nat. Inst. Stand. Technol., Gaithersburg, MD, 2005), <http://physics.nist.gov/Handbook>.
- [42] B. K. Sahoo, B. P. Das, and D. Mukherjee, *Phys. Rev. A* **79**, 052511 (2009).
- [43] D. Mukherjee, B. K. Sahoo, H. S. Nataraj, and B. P. Das, *J. Phys. Chem. A* **113**, 12549 (2009).
- [44] B. K. Sahoo, S. Majumder, R. K. Chaudhuri, B. P. Das, and D. Mukherjee, *J. Phys. B* **37**, 3409 (2004).
- [45] R. W. Schmieder, A. Lurio, and W. Happer, *Phys. Rev. A* **3**, 1209 (1971).
- [46] M. Marinescu, H. R. Sadeghpour, and A. Dalgarno, *Phys. Rev. A* **49**, 5103 (1994).
- [47] C. Zhu, A. Dalgarno, S. G. Porsev, and A. Derevianko, *Phys. Rev. A* **70**, 03722 (2004).
- [48] M. S. Safronova, B. Arora, and C. W. Clark, *Phys. Rev. A* **73**, 022505 (2006).

- [49] K. D. Bonin and M. A. Kadar-Kallen, *Phys. Rev. A* **47**, 944 (1993).
- [50] R. F. Gutterres, C. Amiot, A. Fioretti, C. Gabbanini, M. Mazzoni, and O. Dulieu, *Phys. Rev. A* **66**, 024502 (2002).
- [51] W. F. Holmgren, M. C. Revelle, V. P. A. Lonij, and A. D. Cronin, *Phys. Rev. A* **81**, 053607 (2010).
- [52] W. R. Johnson, D. Kolb, and K.-N. Huang, *At. Data Nucl. Data Tables* **28**, 334 (1983).
- [53] K. E. Miller, D. Krause, and L. R. Hunter, *Phys. Rev. A* **49**, 5128 (1994).
- [54] J. Marek and P. Münster, *J. Phys. B: Atom. Molec. Phys.* **13**, 1731 (1980).
- [55] C. Krenn, W. Scherf, O. Khait, M. Musso, and L. Windholz, *Z. Phys. D: At. Mol. Clusters* **41**, 229 (1997).
- [56] M. S. Safronova, W. R. Johnson, and A. Derevianko, *Phys. Rev. A* **60**, 4476 (1999).
- [57] A. Derevianko, W. R. Johnson, M. S. Safronova, and J. F. Babb, *Phys. Rev. Lett.* **82**, 3589 (1999).
- [58] C. Zhu, A. Dalgarno, S. G. Porsev, and A. Derevianko, *Phys. Rev. A* **70**, 032722 (2004).
- [59] A. Derevianko, W. R. Johnson, M. S. Safronova, and J. F. Babb, *Phys. Rev. Lett.* **82**, 3589 (1999).
- [60] L. R. Hunter, D. Krause, S. Murthy, and T. W. Sung, *Phys. Rev. A* **37**, 3283 (1988).
- [61] L. R. Hunter, D. Krause, K. E. Miller, D. J. Berkeland, and M. G. Boshier, *Opt. Commun.* **94**, 210 (1992).
- [62] C. E. Tanner and C. Wieman, *Phys. Rev. A* **38**, 162 (1988).
- [63] R. Marrus, D. McColm, and J. Yellin, *Phys. Rev. A* **147**, 55 (1966).
- [64] M. J. Seaton, *Comp. Phys. Comm.* **146**, 254 (2002).
- [65] B. Arora, M. S. Safronova, and C. W. Clark, *Phys. Rev. A* **76**, 052516 (2007).